Novel PET and Near Infrared Imaging Probes for the Specific Detection of Bacterial Infections Associated With Cardiac Devices

W. Robert Taylor, *Emory University*
Colleen Kraft, *Emory University*
Jonathon Nye, *Emory University*
Kiyoko Takemiya, *Emory University*
Mark Goodman, *Emory University*
Wone Seo, *Emory University*
X Ning, *University of California Berkeley*
X Wang, *University of California Berkeley*
R Mohammad, *University of California Berkeley*
G Joseph, *Emory University*

Only first 10 authors above; see publication for full author list.

Journal Title: JACC-CARDIOVASCULAR IMAGING
Volume: Volume 12, Number 5
Publisher: ELSEVIER SCIENCE INC | 2019-05-01, Pages 875-886
Type of Work: Article
Publisher DOI: 10.1016/j.jcmg.2018.02.011
Permanent URL: https://pid.emory.edu/ark:/25593/vn5pf

Final published version: http://dx.doi.org/10.1016/j.jcmg.2018.02.011

HHS Public Access

Author manuscript

JACC Cardiovasc Imaging. Author manuscript; available in PMC 2020 May 01.

Published in final edited form as:

JACC Cardiovasc Imaging. 2019 May ; 12(5): 875–886. doi:10.1016/j.jcmg.2018.02.011.

Novel PET and near infrared imaging probes for the specific detection of bacterial infections associated with cardiac devices

Kiyoko Takemiya, MD, PhD[1], **Xinghai Ning, PhD**[2], **Wonewoo Seo, PhD**[3], **Xiaojian Wang, PhD**[2], **Rafi Mohammad, PhD**[2], **Giji Joseph, MS**[1], **Jane S. Titterington, MD, PhD**[1], **Colleen S. Kraft, MD**[4], **Jonathan A. Nye, PhD**[3], **Niren Murthy, PhD**[2], **Mark M. Goodman, PhD**[3], and **W. Robert Taylor, MD, PhD**[1,5,6]

[1]Emory University School of Medicine, Department of Medicine, Division of Cardiology

[2]University of California at Berkeley, Department of Bioengineering

[3]Emory University School of Medicine, Department of Radiology and Imaging Sciences, Emory Center for Systems Imaging

[4]Emory University School of Medicine, Department of Pathology and Laboratory Medicine

[5]Atlanta Veterans Affairs Medical Center, Cardiology Division

[6]Emory University School of Medicine and Georgia Institute of Technology, Department of Biomedical Engineering

Abstract

Objective—To develop imaging agents to detect early stage infections in implantable cardiac devices.

Background—Bacteria ingest maltodextrins through the specific maltodextrin transporter. We developed probes conjugated with either a fluorescent dye (maltohexaose fluorescent dye probe) or a F-18 (F18 Fluoro-maltohexaose) and determined their utility in a model of infections associated with implanted cardiac devices.

Methods—Stainless steel mock-ups were used to model subcutaneous generators were implanted in rats. On postoperative day 4, animals were injected with either *Staphylococcus aureus* around the mock-ups to induce a relatively mild infection or oil of turpentine to induce non-infectious inflammation. Animals with a sterile implant were used as controls. On postoperative day 6, either the maltohexaose fluorescent dye probe or F18 Fluoro-maltohexaose was injected intravenously,

Co-Corresponding authors: W. Robert Taylor MD, PhD, Department of Medicine, Division of Cardiology, Emory University SOM, 101 Woodruff Circle, Suite 319 WMB, Atlanta GA 30322, Tel: 404-727-3754, wtaylor@emory.edu; Niren Murthy, PhD, Department of Bioengineering, UC Berkeley, 284 Hearst Memorial Mining Bldg., Berkeley, CA 94720, Tel: 510-664-4577, nmurthy@berkeley.edu; Mark Goodman, PhD, Center for Systems Imaging, Department of Radiology, and Imaging Sciences, Emory University, 1841 Clifton Rd, NE, WWHC209, Atlanta, GA 30329, Tel: 404-712-9366, mgoodma@emory.edu.

Disclosures

WRT, MG, NM and KT are listed as inventors of the maltodextrin imaging agents under a patent application held by Emory University and the Georgia Institute of Technology.

and the animals were scanned with the appropriate imaging device. Additional PET imaging studies were performed with F18-FDG as a comparison of the specificity of our probes (n= 5 to 9/group).

Results—The accumulation of the maltohexaose fluorescent dye probe in the infected rats was significantly increased at 1 hour after injection when compared to the control and non-infectious inflammation groups (intensity ratio 1.54 ± 0.07 vs 1.26 ± 0.04 and 1.20 ± 0.05 respectively, $P<0.05$) and persisted for over 24 hours. In PET imaging, both F18 Fluoro-maltohexaose and FDG significantly accumulated in the infected area 30 minutes after the injection (SUVmax ratio 4.43 ± 0.30 and 4.87 ± 0.28 respectively). In control rats, there was no accumulation of imaging probes near the device. In the non-infectious inflammation rats, no significant accumulation was observed with F18 Fluoro-maltohexaose, but FDG accumulated in the mock-up area (SUVmaxratio 2.53 ± 0.39 vs 4.74 ± 0.46 respectively, $p<0.05$).

Conclusion—Our results indicate that maltohexaose based imaging probes are potentially useful for the specific and sensitive diagnosis of infections associated with implantable cardiac devices.

Graphical abstract

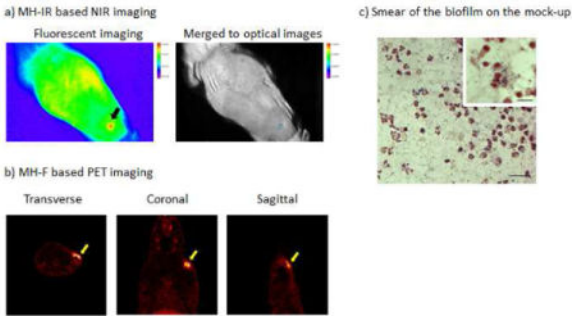

Keywords

Medical Device Infections; Bacterial Imaging; PET; Optical Imaging

Introduction

Implantable cardiac devices such as prosthetic cardiac valves, pacemakers and ICDs, are growing in use due to increases in disease burden and expanded indications.(1,2) Among these devices, the most common cardiac devices are CIEDs which include pacemakers and ICDs. In the United States the number of cardiac devices implanted annually increased from approximately 350,000 to greater than 560,000 over a five year period.(2,3) While these medical devices provide enormous clinical benefit, there is a clear risk of device infections. The incidence of device infection after the primary pacemaker or ICD implantation is approximately 0.5%, but increases by up to 10-fold after device replacement or upgrade surgery.(3)

The clinical assessment of infections associated with CIEDs can be difficult due to nonspecific foreign body inflammation that may masquerade as infection.(4) In addition, the diagnosis is often made after there has been extensive local infiltration a or loss of skin

integrity.(3,5–7) If the diagnosis of existence of bacteria in the skin pocket could be made definitively at an earlier time-point in the postoperative period (particularly in patients at high risk for infection), this could potentially lead to more effective prevention and treatment of the infection that could reduce extraction of CIEDs.

We sought to develop a strategy to detect infections associated with implantable cardiac devices as well as other implantable medical devices. To this end, we identified the maltodextrin transporter for targeting bacteria because of its high uptake (Vmax of 3.3 nmol/min/10^9 cells), and excellent specificity for bacteria.(8) Also, maltodextrins are likely to be cleared from uninfected tissues due to their hydrophilic neutral composition. The maltodextrin transport system is only functional in bacteria.(9) Imaging agents based on maltodextrins also have high translational potential because maltodextrins are commonly used food additives with minimal known toxicity in humans. Finally, the maltodextrin transporter only recognizes the first two sugars of a maltodexrin and is thus relatively insensitive to modifications of the remaining sugars. This potentially permits the addition of an imaging molecule tag onto a maltodextrin without significantly affecting its uptake.(8–10)

With these concepts in mind, we developed two forms of maltohexaose-based imaging probes which have maltohexaose, a maltodextrin consisting of six glucose molecules, as the basic bacterial targeting unit. The first maltohexaose-based imaging probe that we developed is a maltohexaose-based near infrared fluorescent dye imaging probe, which is synthesized by conjugating the near infrared dye, IR-786 to maltohexaose (figure 1A).(8) The maltohexaose fluorescent dye probe is detectable through the skin because light in the near-infrared range is able to penetrate tissue up to several centimeters.(8,11) As generators of CIEDs are located in the subcutaneous layer, the use of maltohexaose fluorescent dye probe seems to be a plausible approach to detect pocket infections using commercially available near infra-red imaging devices as a low cost and as a point of care diagnostic method. The second imaging agent that we developed is a F-18 conjugated maltohexaose, F18 fluoro-maltohexaose (figure 1B), which incorporates ^{18}F as a radioactive tracer for PET imaging.(12) F18 fluoro-maltohexaose PET imaging permits detection of device infections in the deep organs. In this study, we demonstrate that these two probes are able to detect bacterial infections in a sensitive and specific manner and that this unique approach represents a novel diagnostic strategy for the detection of existence of bacteria in an animal model of device pocket infection.

Materials and Methods

The maltohexaose fluorescent and F18 fluoro-maltohexaose probes were synthesized following previously described procedures. (8,12) Briefly, the maltohexaose fluorescent dye probe was synthesized by using “click chemistry” in which maltohexaose with an azide linker was conjugated with a polyethylene glycol linker-added to IR-786 (a near-infrared dye with excitation and emission wavelengths of 710/790 nm).(8) F18 fluoro-maltohexaose was synthesized by one-step nucleophilic 18F fluorination of brosylate-maltohexaase.(12)

Maltohexaose fluorescent dye probe uptake and retention by Staphylococcus aureus in vitro

To determine if the maltohexaose fluorescent dye probe was internalized by MSSA as well as the washout kinetics, 1×10^8 CFU/ml of MSSA (pulse-field gel electrophoresis typed as USA200) was cultured in LB broth with 20 μmol/l of maltohexaose fluorescent dye probe for 1 hour at 37°C. LamB mutant *E. coli* (JW3992–1) which has a mutation in the LamB protein resulting in the dysfunction of maltodextrin transportation system was used as a control. The bacteria were cultured 18 hours and the plates were imaged (In-Vivo Xtreme, Bruker).

To evaluate if the internalized fluorescent probe could be washed out from the bacteria, 20ml of 1×10^8 CFU/ml of MSSA was cultured in LB broth with 20 μmol/l of maltohexaose fluorescent dye probe for 1 hour at 37°C. The bacteria were centrifuged at 10,000×G for 10 min, washed 3 times with fresh LB broth, then re-suspended in the same dose of fresh LB broth. The re-suspended bacteria were aliquoted and incubated at 37°C. At the specified times, bacteria were centrifuged at 10000 xG for 10 min, washed 3 times with PBS, then re-suspended in PBS to evaluate the concentration of maltohexaose fluorescent dye probe (n=3 to 4/time point).

CIED pocket infection and non-infectious inflammation rat models

All animal protocols were approved by the Emory University Institutional Animal Care and Use Committee. Male Sprague-Dawley rats (200–250g, Jackson laboratory ME, U.S.A.) were anesthetized with 1–2% isoflurane, and surgical grade stainless steel mock-ups (5 × 7 × 2 mm) were implanted subcutaneously in the center of the back. On POD 4, rats were divided into 3 groups: an infection group injected with 1×10^9 CFU/0.1ml of MSSA around the mock-up,(13) a non-infectious inflammation group injected with 20 μl of purified oil of turpentine (Sigma Aldrich, MO, U.S.A.) around the mock-up as a model of sterile inflammation, and a control group that did not receive any additional treatment. The dose of MSSA was chosen to induce a relatively minor infection without rubefaction and swelling of the infected site or other systemic signs, which was intended to mimic an early stage, subclinical pocket infection. Fluorescent or PET imaging was performed on POD 6.

Fluorescent Imaging

On POD 6, Rats were anesthetized with isoflurane and injected with 250 μl of 1 mmol/l of the fluorescent dye probe via the tail vein (n= 6 to 9 per group). The animals were scanned with the fluorescent imaging device at the indicated times after injection of the probe and sacrificed at 24 hours for histological study. Gram staining was used to evaluate for the presence of bacteria.

In some cases, cultures were obtained to quantify the level of infection. To quantify the intensity of accumulation of the probe, ROIs were set around the mock-ups, and the fluorescent intensity in the ROIs and that in the entire dorsum of the animal was measured. Data were analyzed as an intensity ratio which was defined as (the mean intensity in the mock-up area) / the mean intensity in the normal skin area (arbitrary units).

PET imaging

On POD 6, (n=5 - 6 per group) rats were anesthetized with isoflurane and either 250 μCi of F18 Fluoro-maltohexaose or 250 μCi of FDG was injected via tail vain. The rats were scanned with a micro-PET/CT (Inveon Micro-PET/CT, Siemens). For quantitative analysis transverse images 30 min after injection of F18 Fluoro-maltohexaose were used and the ROIs were set around the mock-up area and the normal skin area on the dorsum of the animals, contralateral to the side of the mock-ups. Quantitative assessment was made using standard uptake values (SUVs) in the ROI using SUVmean which is defined as [(the mean radioactivity in the ROI)/ (the volume of ROI)]/[(administrated radioactivity)/(body weight)] and SUVmax defined as (the highest pixel value in the ROI)/ [(administrated radioactivity)/ (body weight)]. Data were analyzed using the ratios of the SUV in order to account for differences in body weight as previously described.(14,15)

Biofilm model

Stainless-steel mock-ups were implanted subcutaneously in the center of the back 10 to 14 days before inoculation. At this time point, fibrous pockets were fully formed around the mock-ups and MSSA colonies consisting of bacteria embedded in matrix cultured on LB agar plates placed on the mock-ups through a 24G plastic catheter. In this model, the bacteria are embedded in acellular matrix which mimics a biofilm on an implanted generator and do not spread into surrounding tissues. Two days after inoculation, the rats were imaged as described above for fluorescent (n=7) or PET/CT imaging (n=3).

Biodistribution of maltohexaose fluorescent dye probe

Healthy rats were injected with 250 μl of 1mM dye probe via the tail vein and kept in metabolic cages to collect the feces and urine for 24 hours (n=4). Blood and tissue were harvested using standard techniques. The amount of probe in the organs was calculated based on the concentrations in the sample and quantified as the percent of injected dye.

Statistical Analysis

Analysis was performed with Prism statistical software. For comparison of two groups, Student's T test was used, and one way ANOVA with Tukey's multiple comparison test was used for multi-group comparison. $P<0.05$ was regarded as significant, and all data are shown as mean ± standard error.

Results

MDP is effectively taken up and retained by Staphylococcus aureus in vitro

MSSA internalized the maltohexaose fluorescent dye probe after 1 hour, and the probe remained internalized in MSSA for at least six hours (figure 2). In contrast, LamB mutant bacteria, which lack the maltodextrin transporter, internalized almost no dye probe as indicated by very little fluorescent signal (figure 2). In the quantitative analysis (figure 2C), 1×10^8 CFU of MSSA internalized $1.52 \pm 0.54 \times 10^2$ pmol of maltohexaose fluorescent dye probe in 1 hour. Importantly, the concentrations of fluorescent dye in MSSA showed no significant reduction in intensity over 24 hours indicating retention of the imaging agent.

These data demonstrate that the maltohexaose fluorescent dye probe is internalized by MSSA very specifically through the maltodextrin transport system and is a stable fluorescent imaging agent for bacteria.

Fluorescent imaging

The potential utility of maltohexaose fluorescent dye probe to detect bacterial infection with high sensitivity and specificity was evaluated using a rat model. Rats injected with bacteria exhibited no obvious signs of infection at the site of the device implantation. As shown in figure 3A, the maltohexaose fluorescent dye probe accumulated around the mock-up area in the infection group as soon as 1 hour after injection of the dye probe and persisted for at least 24 hours. Conversely, no significant accumulation of the dye probe was found in either the control group or in the non-infectious inflammation group. In the quantitative analysis (figure 3B), the intensity ratio, which indicates the relative accumulation of probe in the infected mock-up area compared to that in the normal skin area was 1.54 ± 0.07 at 1 hour after the injection of maltohexaose dye probe, and was significantly higher than the non-infectious inflammation group and the control group (1.20 ± 0.05 and 1.28 ± 0.04 respectively, $P<0.05$). No significant difference was found between the non-infectious inflammation group and the control group thus demonstrating specificity of the maltohexaose fluorescent dye probe to detect infection as opposed to inflammation. These data indicated that the maltohexaose fluorescent dye probe accumulated in the site of infection in a highly specific manner with an excellent signal to noise ratio. Conversely, in the non-infectious inflammation model, there was no significant accumulation of the dye probe in the mock-up area.

Histological analysis of the tissue adjacent to the site of implantation of the mock-ups confirmed the presence of bacteria in the infected group as well as sterility in the control and the non-infectious inflammation groups (figure 4). At the time of imaging, the total bacterial burden was 2.9×10^8 CFU (n=4). There was an intense inflammatory response in turpentine treated animals (figure 4). These same animals demonstrated no significant uptake of maltohexaose dye probe.

PET imaging

We also developed a PET imaging agent employing the same targeting strategy in order to image infections in deeper tissues. We examined the sensitivity and the specificity of F18 fluoro-maltohexaose and compared it to FDG. The averages of SUVmean of the normal skin area of all animals were 0.205 ± 0.028 in F18 fluoro-maltohexaose PET imaging and 0.835 ± 0.04048 in FDG PET imaging, indicating the low metabolism and the rapid clearance of F18 fluoro-maltohexaose in animals. As shown in figure 5, both F18 fluoro-maltohexaose and FDG demonstrated significant accumulation around the mock-ups in the infection group (SUVRmean 2.87 ± 0.206 and 2.86 ± 0.26 respectively and SUVRmax 4.43 ± 0.30 and 4.87 ± 0.28 respectively), and neither showed any significant accumulation of tracer in around the mock-ups in the control group. However, in the non-infectious inflammation group, F18 fluoro-maltohexaose showed no significant accumulation around the mock-ups whereas FDG accumulated around the mock-ups (SUVRmean 1.26 ± 0.11 and 2.62 ± 0.28 respectively and SUVRmax 2.53± 0.39 and 4.74 ± 0.46 respectively). The findings with

FDG are consistent with common clinical observations of poor specificity of FDG in this setting due to the lack of ability to discern between inflammation and infection.

Detection of bacteria in a biofilm

We evaluated the ability of our maltodextrin-based imaging probes to detect bacteria embedded in a biofilm. The amount of MSSA delivered to the mockups ranged from 7.3×10^6 to 6.6×10^7 CFU (mean $2.3 \pm 1.2 \times 10^7$ CFU) as the precise amount of bacteria implanted could not be pre-determined. At the time of imaging, the total bacterial burden had decreased to $6.3 \pm 4.6 \times 10^5$ CFU. In histological evaluation, no invasion of bacteria outside of the fibrous pocket was found, but in the smear made with the tissue attached to the mock-ups, scattered Gram positive cocci with neutrophils and macrophages were observed, demonstrating the existence of biofilm similar to that seen in the clinical setting. Despite this modest bacterial burden and the presence of a biofilm, both the maltohexaose fluorescent dye and the F18 fluoro-maltohexaose PET imaging probes were able to detect bacteria in this in vivo model of a biofilm (figure 6).

Biodistribution of the maltohexaose fluorescent dye probe

The distribution of maltohexaose fluorescent dye probe was evaluated in the healthy rats. Twenty four hours after injection of the maltohexaose dye probe, 45.5 ±6.7 % of the injected probe was excreted into the feces, and only 0.4 ± 0.1 % was excreted into urine. The maltohexaose fluorescent dye probe was primarily found in the liver and maltohexaose fluorescent dye probe in the kidneys was low (3.8 ± 0.7 % and 1.1 ± 0.2 %, respectively). The concentration of maltohexaose fluorescent dye probe in the intestine was 0.52 μM, (1.2 ± 0.5 % of injected probe). Other organs, such as the spleen, the heart and the lungs, contained less than 1% of injected probe. Other tissue, such as the muscles and the skin, contained small amount of maltohexaose fluorescent dye probe below the level of quantitative detection. Because of the short half-life of F18, we did not evaluate the distribution of F18 fluoro-maltohexaose 24 hours after injection. However, significant accumulation of tracer was found in the bladder, indicating that F18 fluoro-maltohexaose is excreted primarily into the urine at these early time points.

Discussion

In this study, we present robust preclinical data demonstrating the utility of targeting the maltodextrin transporter to identify the presence of bacteria in a very sensitive and specific manner. We demonstrated that both the maltohexaose fluorescent dye and F18 fluoro-maltohexaose probes were able to detect very early stage bacterial infections in a model of subclinical infection of device pocket infection in rats.

The diagnosis of pocket infection related to cardiac devices is an important clinical problem in medicine today. Due to the expanding use of implantable medical devices, the large number of immunocompromised patients, an aging population, and the emergence of drug resistant bacteria, the number of patients with infected medical devices continues to grow. (1,2,16) The number of hospital admissions for CIED infections has increased 3-fold over an eight year period, paralleling a similar increase in the number of device infections.

Importantly, pocket infections are associated with at least a doubling of mortality.(17) The incremental cost associated with infection of an implantable electronic cardiac device is estimated to be in excess of $50,000 per patient.(18)

In our experiments, we intentionally performed the in vivo studies using a very mild degree of infection in order to mimic a pre-clinical infection. The infected animals exhibited no overt signs of infection at the site of the infected mock-ups and had no systemic signs of infection. We undertook this strategy in order to test the ability of maltohexaose based imaging probes to detect bacteria at a stage of infection that is clinically challenging. This raises the possibility that in select patients with early stage infection, there exists the possibility to effectively treat the infection with antibiotics without the need to extract the device. In addition, our approach to bacterial imaging could also be used to monitor the efficacy of antibiotic therapy. The impact of this approach on morbidity and mortality as well as the costs associated with infected medical devices could be very significant.

Our studies demonstrated that the maltohexaose fluorescent dye probe was internalized by MSSA and that the accumulated fluorescent maltohexaose fluorescent dye probe remained in MSSA without a loss of the fluorescent activity. MSSA was employed in this study because it is one of the most common causes of the pocket infections. However, the maltodextrin transport system exists universally in all bacteria, and we have previously shown that a maltodextrin conjugated dye probe is internalized by many species of bacteria.(8) These characteristics make a maltohexaose fluorescent dye probe potentially very useful in many clinical applications because of the persistence of the signal and the ability to detect a wide range of bacteria.

We also showed that maltohexaose fluorescent dye probe detected subclinical bacterial pocket infections in rats with high sensitivity and high specificity employing near infrared fluorescent imaging. Optical imaging strategies in general are limited by the ability to detect the probes in deeper tissues. However, the use of near infrared dyes mitigates this limitation to some degree as detection up to several centimeters is possible with commercially available equipment.(19) In the specific case of CIEDs, there is the advantage that the generator is generally located in the subcutaneous space near the surface of the skin. Although the leads of CIEDs are significantly deeper in the body, and infection at these sites would not be readily detected by surface optical imaging strategies, the majority of CIED infections involve the generator and pocket.(3) Even though the sensitivity of maltohexaose fluorescent dye probe is very likely less than that of F18 fluoro-maltohexaose, the maltohexaose fluorescent dye probe still has sufficient sensitivity to detect the existence of very small amounts of bacteria. Furthermore NIR imaging is less expensive than PET imaging and could be employed at the bedside without the need for extremely expensive imaging equipment. This may be particularly useful in those patients at increased risk for infections associated with CIEDs (e.g., diabetics, patients on hemodialysis, etc.).

We also developed a PET imaging-based strategy using F18 fluoro-maltohexaose that is similarly very sensitive and specific for detecting the existence of bacteria. This imaging agent is superior to FDG due to its ability to distinguish bacterial infection from sterile inflammation in vivo. Although PET imaging requires dedicated facilities and higher cost

than fluorescent imaging, the improved sensitivity of PET imaging may ultimately prove to be very beneficial.

The use of imaging agents to effectively detect localized bacterial infections has been the goal of several previous investigations. Sarrazin et al originally reported that FDG PET imaging was effective in the diagnoses of skin pocket infection with approximately 90% of specificity.(4) An important difference between their study and ours is that we were able to discern between intense sterile inflammation and true infection with the maltohexaose-based probes. For both the fluorescent and PET imaging probes, no significant uptake was observed in the turpentine model of sterile inflammation. This was in contrast to the positive uptake observed with FDG imaging of sterile inflammation. These results support the main thesis of our study that maltohexaose based imaging probes are specifically internalized by bacteria and that because of the increased specificity and sensitivity, these novel imaging agents may prove to be a valuable tool to image bacterial infections associated with implantable cardiac devices.

Recently, Zhang et al studied the ability of radioactively labelled fialuridine, [^{124}I]FIAU (a nucleoside analog which is a substrate for bacterial thymidine kinase) to detect bacterial infections associated with prosthetic joints. Despite promising preclinical studies, the human studies failed to demonstrate efficacy of this approach.(20) A major contributor to the failure of their studies was the non-specific muscle uptake of FIAU.(20) In contrast to [^{124}I]FIAU, the advantage of F18 fluoro-maltohexaose is that there is very likely markedly lower non-specific uptake by mammalian tissues.

Employing the same approach of targeting the maltodextrin transporter as we initially described(12), Gowrishankar et al reported that F18 labeled fluoromaltose was able to detect bacterial infections caused by E. coli in a mouse thigh abscess model.(21) Subsequent work by the same group reported on the development of a related compound, 18F-fluoromaltotriose which possesses improved urinary clearance when compared to their original fluoromaltose imaging agent.(22) A comparison of imaging efficacy was not carried out. These studies support the overall concept of targeting the maltodextrin transporter and raise that possibility that these or other modifications may impact the biodistribution and potentially the efficacy.

The potential application of these imaging probes extends beyond the ability to diagnose device pocket infections. Although there may be issues with gating and subsequent spatial resolution of cardiac structures, these agents could potentially be used to diagnose endocarditis of native or prosthetic heart valves as well as infections associated with LVADs and other cardiovascular implants. Maltodextrin-based imaging agents may be useful in other clinical settings as well including infections associated with orthopedic implants, identifying the source of bacteremia, diagnosing bacterial infections of the lungs, etc. Moreover, it is suggested that our strategy of specific molecular delivery to bacteria with maltohexaose could be a platform for targeting therapeutics to bacteria or could potentially be expanded as a “theranostic” in order to image bacteria and simultaneously directly target anti-bacterial agents.

Conclusion

Targeting the maltodextrin transporter is an effective strategy for delivering imaging agents to bacteria in order to diagnose and localize bacterial infections. We developed both fluorescent and PET imaging agents that are potentially useful for the specific diagnosis of bacterial infections associated with implanted cardiac devices. This strategy has the potential to positively impact the morbidity and mortality as well as the healthcare costs associated with infections of implanted medical devices. Moreover, our study suggests that maltodextrins can be molecular vectors specific for bacteria with broader applications for the diagnosis and treatment of bacterial infections.

Acknowledgments

Funding Sources

This work was supported by NIH 1R01EB020008, a generous gift from the John and Mary Brock Innovation Fund and Funding from the Georgia Research Alliance.

Abbreviations

CIEDs	cardiovascular implantable electronic devices
CFU	colony forming units
FGD	F-18 fluorodeoxyglucose
ICDs	implantable cardioverter-defibrillators
LB	broth Luria-Bertani broth
MSSA	methicillin sensitive *Staphylococcus aureus*
PET	positron emission tomography
POD	post-operative day
ROI	region of interest
SUVmax	maximum standard uptake value
SUVmean	mean standard uptake value
SUVRmax	Ratio of SUVmax
SUVRmean	Ratio of SUVmean

References

1. Olsen NT, De Backer O, Thyregod HG, et al. Prosthetic valve endocarditis after transcatheter aortic valve implantation. Circ Cardiovasc Interv. 2015; 8
2. Greenspon AJ, Patel JD, Lau E, et al. 16-year trends in the infection burden for pacemakers and implantable cardioverter-defibrillators in the United States 1993 to 2008. Journal of the American College of Cardiology. 2011; 58:1001–6. [PubMed: 21867833]

3. Tarakji KG, Wilkoff BL. Management of cardiac implantable electronic device infections: the challenges of understanding the scope of the problem and its associated mortality. Expert review of cardiovascular therapy. 2013; 11:607–16. [PubMed: 23621142]
4. Sarrazin JF, Philippon F, Tessier M, et al. Usefulness of fluorine-18 positron emission tomography/computed tomography for identification of cardiovascular implantable electronic device infections. Journal of the American College of Cardiology. 2012; 59:1616–25. [PubMed: 22538331]
5. Nataloni M, Pergolini M, Rescigno G, Mocchegiani R. Prosthetic valve endocarditis. Journal of cardiovascular medicine. 2010; 11:869–83. [PubMed: 20154632]
6. Habib G, Hoen B, Tornos P, et al. Guidelines on the prevention, diagnosis, and treatment of infective endocarditis (new version 2009): the Task Force on the Prevention, Diagnosis, and Treatment of Infective Endocarditis of the European Society of Cardiology (ESC). Endorsed by the European Society of Clinical Microbiology and Infectious Diseases (ESCMID) and the International Society of Chemotherapy (ISC) for Infection and Cancer. European heart journal. 2009; 30:2369–413. [PubMed: 19713420]
7. Chen W, Kim J, Molchanova-Cook OP, Dilsizian V. The potential of FDG PET/CT for early diagnosis of cardiac device and prosthetic valve infection before morphologic damages ensue. Curr Cardiol Rep. 2014; 16:459. [PubMed: 24482013]
8. Ning X, Lee S, Wang Z, et al. Maltodextrin-based imaging probes detect bacteria in vivo with high sensitivity and specificity. Nature materials. 2011; 10:602–7. [PubMed: 21765397]
9. Gopal S, Berg D, Hagen N, et al. Maltose and maltodextrin utilization by Listeria monocytogenes depend on an inducible ABC transporter which is repressed by glucose. PloS one. 2010; 5:e10349. [PubMed: 20436965]
10. Dahl MK, Manson MD. Interspecific reconstitution of maltose transport and chemotaxis in Escherichia coli with maltose-binding protein from various enteric bacteria. Journal of bacteriology. 1985; 164:1057–63. [PubMed: 3905762]
11. Hilderbrand SA, Weissleder R. Near-infrared fluorescence: application to in vivo molecular imaging. Current opinion in chemical biology. 2010; 14:71–9. [PubMed: 19879798]
12. Ning X, Seo W, Lee S, et al. PET imaging of bacterial infections with fluorine-18-labeled maltohexaose. Angew Chem Int Ed Engl. 2014; 53:14096–14101. [PubMed: 25330976]
13. Tseng CW, Sanchez-Martinez M, Arruda A, Liu GY. Subcutaneous infection of methicillin resistant Staphylococcus aureus (MRSA). Journal of visualized experiments : JoVE. 2011
14. Boellaard R, Delgado-Bolton R, Oyen WJ, et al. FDG PET/CT: EANM procedure guidelines for tumour imaging: version 2.0. Eur J Nucl Med Mol Imaging. 2015; 42:328–54. [PubMed: 25452219]
15. Johnsrud K, Skagen K, Seierstad T, Skjelland M, Russell D, Revheim ME. (18)F-FDG PET/CT for the quantification of inflammation in large carotid artery plaques. J Nucl Cardiol. 2017
16. Tarakji KG, Chan EJ, Cantillon DJ, et al. Cardiac implantable electronic device infections: presentation, management, and patient outcomes. Heart rhythm : the official journal of the Heart Rhythm Society. 2010; 7:1043–7.
17. Baddour LM, Epstein AE, Erickson CC, et al. Update on cardiovascular implantable electronic device infections and their management: a scientific statement from the American Heart Association. Circulation. 2010; 121:458–77. [PubMed: 20048212]
18. Sohail MR, Henrikson CA, Braid-Forbes MJ, Forbes KF, Lerner DJ. Mortality and cost associated with cardiovascular implantable electronic device infections. Archives of internal medicine. 2011; 171:1821–8. [PubMed: 21911623]
19. Kitai T, Inomoto T, Miwa M, Shikayama T. Fluorescence navigation with indocyanine green for detecting sentinel lymph nodes in breast cancer. Breast Cancer. 2005; 12:211–5. [PubMed: 16110291]
20. Zhang XM, Zhang HH, McLeroth P, et al. [(124)I]FIAU: Human dosimetry and infection imaging in patients with suspected prosthetic joint infection. Nucl Med Biol. 2016; 43:273–9. [PubMed: 27150029]
21. Gowrishankar G, Namavari M, Jouannot EB, et al. Investigation of 6-[(1)(8)F]-fluoromaltose as a novel PET tracer for imaging bacterial infection. PloS one. 2014; 9:e107951. [PubMed: 25243851]

22. Gowrishankar G, Hardy J, Wardak M, et al. Specific Imaging of Bacterial Infection Using 6″-(18)F-Fluoromaltotriose: A Second-Generation PET Tracer Targeting the Maltodextrin Transporter in Bacteria. J Nucl Med. 2017; 58:1679–1684. [PubMed: 28490473]

Perspectives

Competency In Medical Knowledge

The accurate diagnosis of bacterial infections associated implanted medical with remains a significant medical that continues to grow as our population ages and the indications for these devices broaden. Currently available imaging modalities suffer from insufficient diagnostic accuracy and additional approaches are needed.

Translational Outlook

Novel approaches are needed to identify infections associated with medical devices as current methods of imaging white blood cells have inherent limitations. The maltodextrin transporter is a unique bacterial target that opens up the possibility of developing a family of highly specific imaging agents for bacteria.

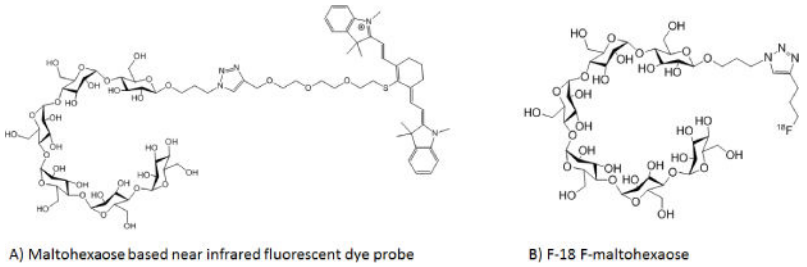

Figure 1. Structures of Imaging Agents

A) Structural formula of maltohexaose-based near infrared fluorescent dye probe and **B)** F18 fluoro-maltohexaose.

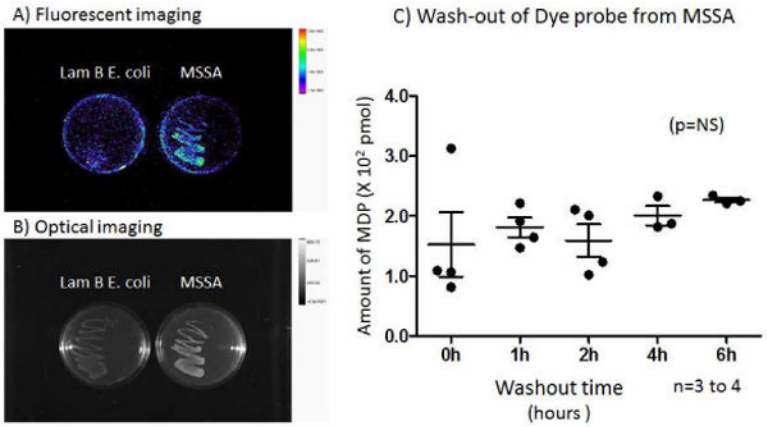

Figure 2. Specific uptake of maltohexaose fluorescent dye probe by bacteria

1×10^8/CFU/ml of MSSA or Lam B mutant *E. coli* were cultured with 20μM of maltohexaose fluorescent dye probe for 1 hour. **(A)** MSSA exhibited a clear signal whereas Lam B mutant E. coli had very little uptake of the dye probe. Note that there is some autofluorescence from the plastic culture dish. **B)** Optical imaging demonstrating similar bacterial density. **C)** 1×10^8/CFU/ml of MSSA was cultured with 20 mol/l of maltohexaose fluorescent dye probe for 1 hour and washed. The bacterial culture was incubated LB broth without maltohexaose fluorescent dye probe, washed again, and the remaining maltohexaose fluorescent dye probe in bacteria quantified. 1×10^8/CFU of MSSA internalized $1.52 \pm 0.54 \times 10^2$ pmol of maltohexaose fluorescent dye probe in 1 hour, and the concentrations of fluorescent dye in MSSA showed no significant changes for up to 6 hours. n = 3 to 4/time point.

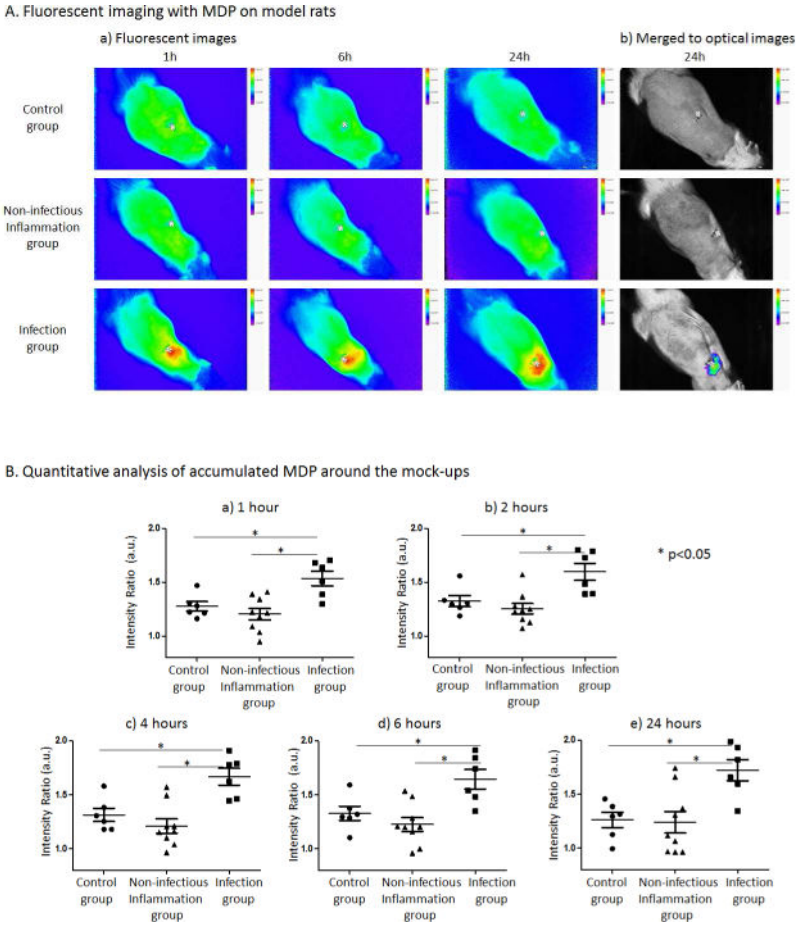

Figure 3. Fluorescent imaging with maltohexaose fluorescent dye probe in vivo

A) Robust accumulation of maltohexaose fluorescent dye probe was seen around the mock-up in the infection group as soon as 1 hour after the injection of the dye probe, while no significant accumulation was observed in the non-infectious inflammation group and in the control group. **B)** The corrected intensity ratios in the infection group were significantly increased compared to those in the non-infectious inflammation group and in the control group at all time points. n = 6 to 9 per group.

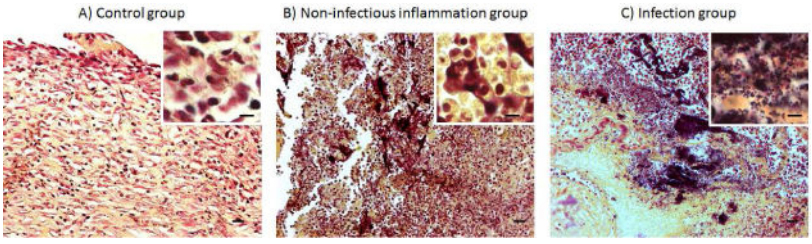

Figure 4. Demonstration of the presence of bacteria in the infected mock-ups

Skin samples around the mock-ups demonstrated an inflammatory response was seen in all groups but was most intense in the inflammation and infection groups. Note that, as expected, gram positive cocci were seen only in the infection group (C). Magnification 20×, bars 20 μm. Magnification in the inset 100×, bars 5μm.

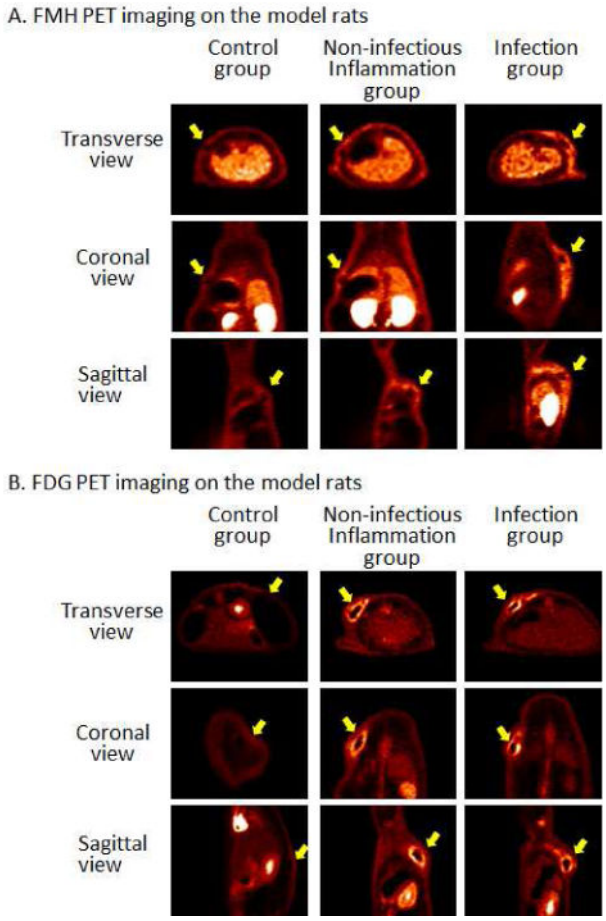

Figure 5. FMH and FDG PET imaging in vivo

(A) F18 fluoro-maltohexaose accumulation was clearly observed in the infection group with very low accumulation in the control group and in the non-infectious inflammation group. Conversely, with FDG PET imaging (B), the accumulation of radioactivity was observed in the infection group as well as in the noninfectious inflammation group. Yellow arrows indicate the locations of the mock-ups. For F18 fluoro-maltohexaose PET imaging, the infection group had a significant increase in both SUVRmax and SUVRmean when compared to both the control group and the non-infectious inflammation group. With FDG PET imaging, the infection group and the non-infectious inflammation group had a similar, significant increase in both SUVRmax and SUVRmean when compared to the control group demonstrating a lack of specificity (C). N = 5 to 6 per group.

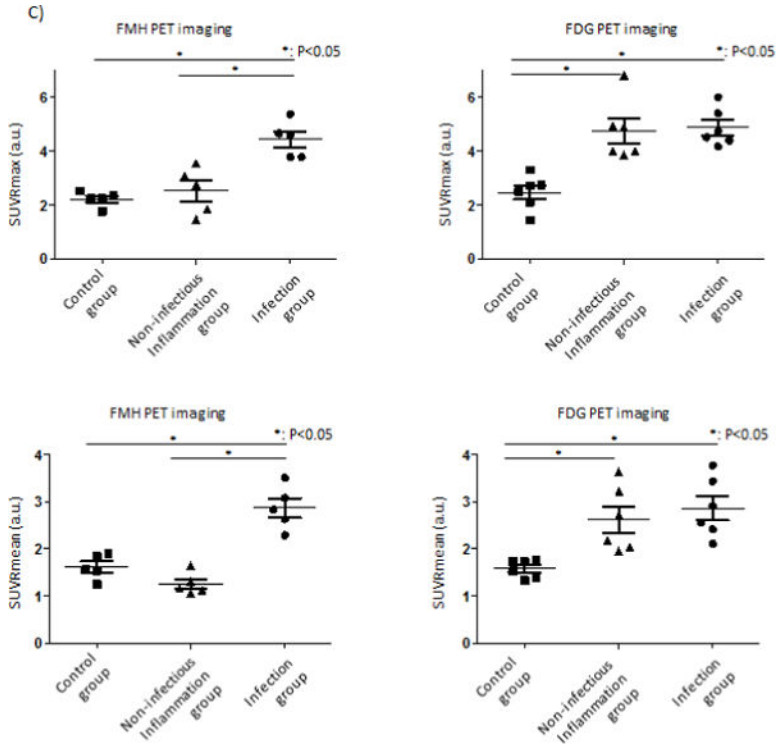

Figure 6. Detection of bacteria in a biofilm on implanted mock-up devices

Rats were implanted with the mock-up devices, and a small amount of biofilm forming MSSA was inoculated on the implanted mock-up devices as a biofilm model. Two days after inoculation, the rats were injected with the maltohexaose fluorescent dye probe or F18 fluoro-maltohexaose via the tail vein. Both the maltohexaose fluorescent dye probe (A) and F18 fluoro-maltohexaose (B) accumulated at the site of the infected mock-up device. Arrows indicate locations of the mock-ups.